Fungal Genetics and Biology 69 (2014) 96–108

Contents lists available at ScienceDirect

Fungal Genetics and Biology

journal homepage: www.elsevier.com/locate/yfgbi

Purine utilization proteins in the Eurotiales: Cellular compartmentalization, phylogenetic conservation and divergence

Katerina Galanopoulou [a], Claudio Scazzocchio [b,c], Maria Eleftheria Galinou [a], Weiwei Liu [b,1], Fivos Borbolis [a], Mayia Karachaliou [a], Nathalie Oestreicher [b,2], Dimitris G. Hatzinikolaou [a], George Diallinas [a,*], Sotiris Amillis [a,*]

[a] Faculty of Biology, University of Athens, Panepistimioupolis, Athens 15784, Greece
[b] Institut de Génétique et Microbiologie, Université Paris-Sud (XI), 91450 Orsay, France
[c] Department of Microbiology, Imperial College London, South Kensington Campus, Flowers Building, Armstrong Road, London SW7 2AZ, UK

ARTICLE INFO

Article history:
Received 29 April 2014
Accepted 10 June 2014
Available online 24 June 2014

Keywords:
Aspergillus nidulans
Uric acid
Peroxisome
Transporter

ABSTRACT

The purine utilization pathway has been thoroughly characterized in *Aspergillus nidulans*. We establish here the subcellular distribution of seven key intracellular enzymes, xanthine dehydrogenase (HxA), urate oxidase (UaZ), 5-hydroxy-isourate hydrolase (UaX), 2-oxo-4-hydroxy-4-carboxy ureido imidazoline decarboxylase (UaW), allantoinase (AlX), allantoicase (AaX), ureidoglycolate lyase (UglA), and the fungal-specific α-ketoglutarate Fe(II)-dependent dioxygenase (XanA). HxA, AlX, AaX, UaW and XanA are cytosolic, while UaZ, UaX and UglA are peroxisomal. Peroxisomal localization was confirmed by using appropriate *pex* mutants. The pathway is largely, but not completely conserved in the Eurotiomycetes, noticeably in some species AaX is substituted by an alternative enzyme of probable bacterial origin. UaZ and the urate–xanthine UapA and UapC transporters, are also localized in specific cells of the conidiophore. We show that metabolic accumulation of uric acid occurring in *uaZ* null mutations is associated with an increased frequency of appearance of morphologically distinct colony sectors, diminished conidiospore production, UV resistance and an altered response to oxidation stress, which may provide a rationale for the conidiophore-specific localization. The pathway-specific transcription factor UaY is localized in both the cytoplasm and nuclei under non-inducing conditions, but it rapidly accumulates exclusively to the nuclei upon induction by uric acid.

1. Introduction

Work starting in the 1960s has led to the identification of all the genes encoding the enzymes of the purine utilization pathway in *Aspergillus nidulans* (Gournas et al., 2011 and refs therein). The pathway of purine utilization in *A. nidulans* is shown in Fig. 1. This conforms to the classical purine degradation pathway (Darlington et al., 1965; Vogels and Van der Drift, 1976; Lehninger, 1981), with the addition that xanthine hydroxylation to uric acid can be catalyzed by, besides xanthine dehydrogenase also by an α-ketoglutarate dependent xanthine di-oxygenase, an exclusive fungal enzyme (Cultrone et al., 2005; Montero-Morán et al., 2007). While the pathway has been thoroughly characterized genetically, physiologically and biochemically in this organism (Gournas et al., 2011 and refs therein), the subcellular localization of purine break down is still unknown. This is of considerable interest, as while the biochemical steps are conserved from bacteria to metazoa (with some interesting bacterial exceptions; De la Riva et al., 2008; Pope et al., 2009), orthologous enzymes involved in purine utilization show variable cell localization throughout the evolutionary tree (Hayashi et al., 2000), raising the question of metabolite transport between cellular compartments. *A. nidulans*, as all the members of the Pezizomycotina, is a multicellular organism, which permits to study the distribution of metabolites among specialized cells. The presence of the specific uric acid–xanthine transporter UapA in the metullae, intermediate cells in the development of conidiospores, suggests that indeed purine derivatives can be transported from one cell type to the other in the conidiophore

* Corresponding authors. Fax: +30 (210)7274702 (S. Amillis).
E-mail address: samillis@biol.uoa.gr (S. Amillis).
[1] Present address: Jubilant HollisterStier, 16751 Trans-Canada Route, Kirkland, Quebec, Canada.
[2] Present address: Pôles Risques MSH-CNRS, Université de Caen, 14032 Caen Cedex, France.

http://dx.doi.org/10.1016/j.fgb.2014.06.005
1087-1845/

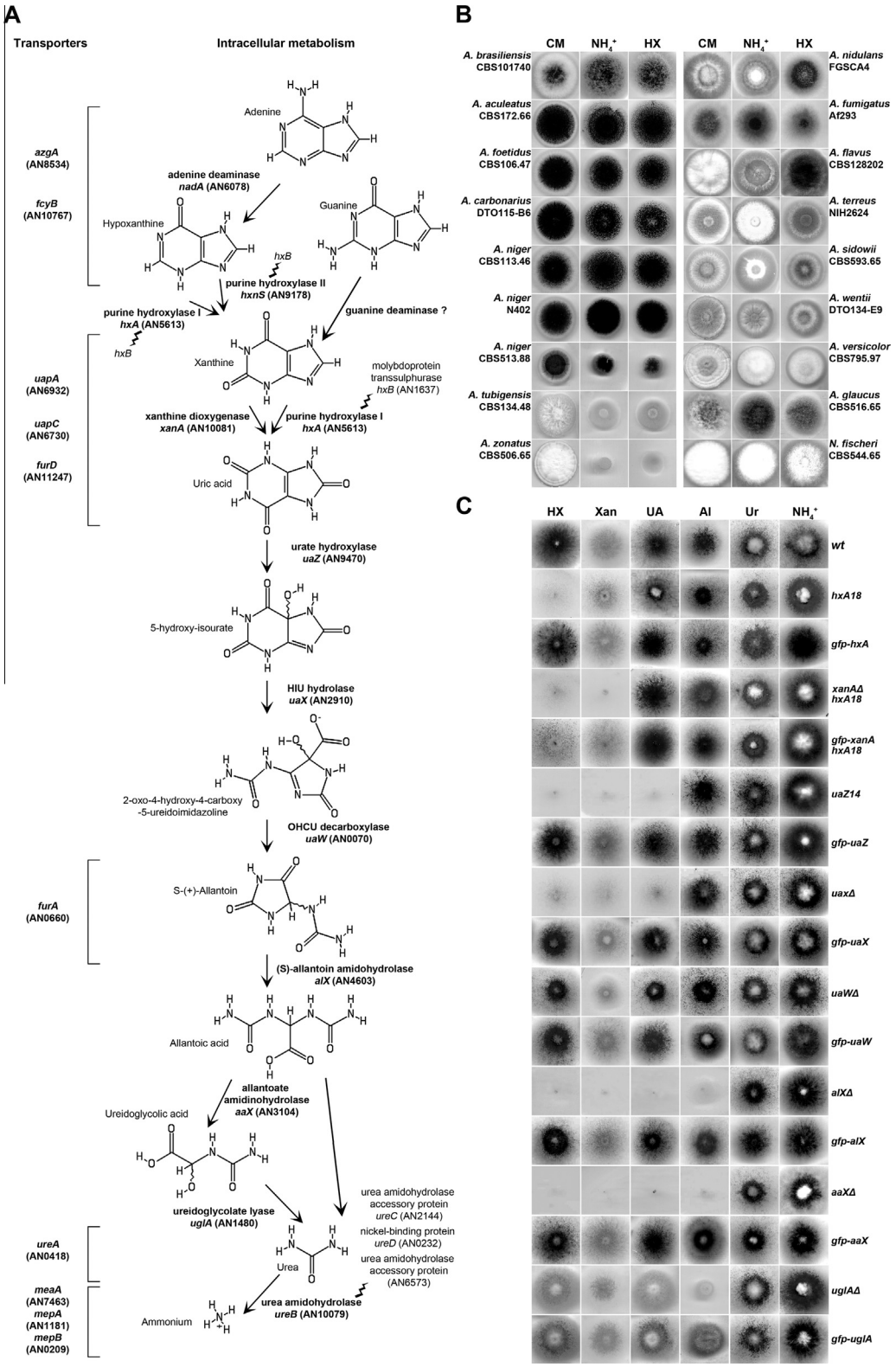

Fig. 1. Gene–enzyme relationships in the purine utilization pathway of Aspergilli and relevant mutant phenotypes in *A. nidulans*. (A) The pathway of purine degradation to ammonium in *A. nidulans* is shown. Adjacent to each arrow the corresponding enzymatic reaction is shown, together with the name and identifier of the cognate gene. The transporters involved in the uptake of different metabolites are also shown to the left of the figure. Connected by a wave-line to the relevant enzymes we show genes and their cognate proteins involved in cofactor synthesis or modification. Experimental identification of each gene is described herein and in a number of publications that are summarized in Gournas et al. (2011). Guanine is a nitrogen source for *A. nidulans* and thus it must be metabolized through this pathway, however, as no experimental work on the conversion of guanine, presumably to xanthine, is extant, nor has a guanine deaminase activity been characterized, a question mark indicates this predicted step. (B) Growth tests of different *wt Aspergillus* species (see Table S3) on complete media (CM) and on minimal media supplemented with ammonium (NH_4^+) or hypoxanthine (HX) as sole nitrogen sources. (C) Growth tests of *A. nidulans* wild-type (*wt*), purine utilization mutants, and purine utilization mutants complemented with *gfp*-tagged versions of the relevant genes, on minimal medium (MM) supplemented with purines or purine-related catabolic metabolites. These are: hypoxanthine (Hx); xanthine (Xan); uric acid (UA); allantoin (Al); urea (Ur) and ammonium (NH_4^+). Growth was carried out at 37 °C, pH 6.8 for 48 h.

(Pantazopoulou et al., 2007). While urate oxidase has been found to be a peroxisomal enzyme in every eukaryote where its localization has been studied, from amoeba (Müller and Moller, 1969) to mammals (Moriwaki et al., 1999), no such general statement could be made about other enzymes of the pathway where variations could be found among different phyla or even within the same phylum (Hayashi et al., 2000). Interestingly, uric acid as the metabolic end product of purine catalysis is an important contributor in the total antioxidant defence in humans, being the major antioxidant present in blood (Yu and Schellhorn, 2013 and refs therein). Metabolically produced uric acid has a similar antioxidant property in *Drosophila melanogaster* (Hilliker et al., 1992). Following the completion of the purine degradation pathway in *A. nidulans* (Gournas et al., 2011), we establish here the intracellular localization of the specific enzymes of the purine utilization pathway in this model organism and we address the problem of the localization of purine metabolites in the conidiophore and of its possible function. The availability of a number of genomes of the Aspergilli and related species allowed to address the conservation of the enzymes of the pathway and to reveal unexpected differences. We also studied the nuclear-cytoplasmic shuffle of the specific purine utilization transcription factor UaY, one of the best-studied transcription factors in the Pezizomycotina (Scazzocchio et al., 1982; Suárez et al., 1995; Oestreicher and Scazzocchio, 1995, 2009; Cecchetto et al., 2012).

2. Materials and methods

2.1. Strains, media, standard genetic techniques and growth conditions

A. nidulans strains used are listed in Table S1. Gene replacement null mutant strains were constructed by transformation of *pyrG89 nkuA*Δ (uracil/uridine auxotrophy and DNA helicase null mutant, respectively; Nayak et al., 2006) strains, using DNA linear cassettes carrying the *A. fumigatus* selection marker AF*pyrG* (Afu2g0836). *hxA18* is a chain termination mutation at codon 148 of the *hxA* gene encoding purine hydroxylase I (Glatigny and Scazzocchio, 1995). *uaZ14* is a chain termination mutation after residue 131 in exon 2 of the *uaZ* gene encoding urate hydroxylase, leading to extremely low mRNA levels and absence of UaZ cross reacting material (CRM) (Oestreicher et al., 1993). *uaZ11* is a I/VIII chromosomal translocation, which splits the *uaZ* gene (Oestreicher and Scazzocchio, 1993; Oestreicher et al., 1993). The loss-of-function mutation *xanA1* is a C to T transition at position +561, resulting in an Ala to Asp change at residue 167 of the XanA protein. Its phenotype is identical to that of a deletion mutation, which was also used in this work (Cultrone et al., 2005). The null mutation *uaY205* corresponds to a 16 bp deletion that results in premature translation termination and substitutes the C-terminal 63 amino acids for 13 new residues (Oestreicher et al., 1997). The loss-of-function allele *uaY808* is a deletion of 484-bp between positions +998 and +1482, associated with an insertion of a sequence of 5 bp (CTCGT). The resulting frame-shift introduces a stop codon, 9 triplets downstream from the end of the deletion (Suárez et al., 1995, N. Oestreicher, unpublished). The gain-of-function allele *uaY462* is a C to T transition in codon 222, resulting in a Ser to Leu change (Oestreicher and Scazzocchio, 1995). Derivatives of mutant strains were made with standard genetic crossing using auxotrophic markers for heterokaryon establishment. *Escherichia coli* DH5α strain was used for routine plasmid preparation and construction. Transformation of *A. nidulans* was performed according to Tilburn et al. (1983) or Koukaki et al. (2003). Growth conditions for *A. nidulans* were according to Scazzocchio et al. (1982). Standard complete (CM) and minimal media (MM) supplemented with appropriate auxotrophies for *A. nidulans* were used (http://www.fgsc.net). Nitrogen sources were used at the final concentrations: urea 5 mM, $NaNO_3$ 10 mM, Ammonium L-(+)-tartrate 10 mM, proline 5 mM, purines 0.6 mM, allantoin 1 mM, allantoic acid 0.5–2 mM. Paraquat was used at a concentration of 0.25 mM, in the presence of urea as sole nitrogen source. Media and chemical reagents were obtained from Sigma–Aldrich or AppliChem. For experiments where the concentration of inoculum was a prerequisite, spore solutions of the corresponding strains were adjusted with the use of a Neubauer plate. UV-survival tests using equal numbers of spores for each strain (10^3 conidiospores) were performed on inoculated solid CM media at a distance of 30 cm from an Osram HNS30 UV-C lamp at 10, 30 or 60 s intervals and then incubated for 48 h. Each condition was performed in triplicate. Colonies were counted and average values were used.

2.2. DNA manipulations and construction of replacement cassettes

Construction of strains containing in-locus translational fusions and relevant plasmids are described in detail in the Supplementary Materials and Methods and Fig. S1.

2.3. Western blot analysis

Total protein extracts were prepared from mycelium in liquid cultures incubated for 14–16 h at 25 °C under non-inducing ($NaNO_3$) or inducing conditions ($NaNO_3$, uric acid) (Apostolaki et al., 2012). In brief, approximately 200 mg of liquid nitrogen grinded mycelia were resuspended in precipitation buffer (50 mM Tris pH 8, 50 mM NaCl, 12.5% TCA) and incubated on ice for 20 min. The suspension was centrifuged for 10 min at 13,000 rpm at 4 °C and the resulting pellet was washed twice with ice cold acetone, air-dried and dissolved in extraction buffer (100 mM Tris pH 8, 50 mM NaCl, 1% SDS, 1 mM EDTA) supplemented with a protease inhibitor cocktail (P8215; Sigma–Aldrich). After centrifugation for 10 min at 13,000 rpm and 4 °C the supernatants were subjected to western blotting analysis. Protein concentrations were determined by the method of Bradford. In each case, 30–50 μg protein, mixed with reducing SDS loading buffer and boiled at 95 °C for 5 min, were fractionated on 10% SDS–PAGE gel and electroblotted (Mini PROTEAN™ Tetra Cell, BIO-RAD) onto PVDF membrane (Macherey–Nagel). Immunodetection was performed using a primary mouse anti-GFP monoclonal antibody (Roche Diagnostics), a mouse anti-actin monoclonal (C4) antibody (MP Biomedicals Europe) and a secondary goat anti-mouse IgG HRP-linked antibody (Cell Signaling Technology Inc.) and detected by the chemiluminescent method using the LumiSensor Chemiluminescent HRP Substrate kit (GenScript USA Inc.).

2.4. Fluorescence microscopy

Vegetative mycelia were grown on cover slips for 14–18 h at 25 °C in MM supplemented with glucose (1% w/v), or fructose (0.1% w/v) as sole carbon sources and urea or $NaNO_3$ as sole nitrogen sources (Gournas et al., 2010). Preparation of samples for the microscopic observation of asexual compartments was performed according to Pantazopoulou et al. (2007). In the case of GFP-tagged versions of enzymes involved in purine catabolism, $NaNO_3$ was used as nitrogen source and uric acid or hypoxanthine was added for induction. Staining with FM4-64 was according to Peñalva (2005). Samples were observed on an Axioplan Zeiss phase-contrast epi-fluorescent microscope and images were acquired with a Zeiss-MRC5 digital camera using the AxioVs40 V4.40.0 software with appropriate filters. For UaY-GFP microscopy, urea was used as sole nitrogen source, whereas for inducing conditions uric acid was added for the last two hours, and for repressing conditions, ammonium tartrate for the last one hour. Samples were observed

on a Nikon Eclipse E400 using appropriate filters and images acquisitions were done on a Nikon Coolpix 8400, using the same setting. Image processing and contrast adjustment were made using the Adobe Photoshop CS4 Extended version 11.0.2 software or the ImageJ software. Images were converted to 8-bit grayscale or RGB and annotated using Photoshop CS4 before being saved to TIFF.

2.5. Uric acid determination by HPLC

Mycelia extracts were prepared as follows: Liquid cultures were left to grow for 12 h at 37 °C. Mycelia were isolated by infiltrating the culture and freezing in liquid nitrogen. To prepare the conidiospore extracts, 15 plates of MM for each strain were incubated for 7 days at 30 °C. Spores were collected in liquid MM and separated from the mycelium by infiltration. Suspensions were centrifuged at 4000 rpm for 15 min, resuspended in MM and centrifuged again for 5 min. Supernatant was discarded and spores were frozen overnight at −80 °C. Frozen mycelia or conidiospores were shattered in liquid nitrogen, their mass was measured in an analytical balance and were suspended in 100 mM $Na_2B_4O_7$ pH 8 to obtain a final concentration of 200 mg/mL. An equal volume of glass beads to that of the shattered mycelium or conidiospores was added and each sample and the mixture was vigorously vortexed for at least 5 min. Samples were centrifuged at 4000 rpm for 15 min and the supernatant was transferred into a new tube for further analysis. For the determination of uric acid concentration in the mycelial and spore extracts through HPLC, a modified version of the method published by Mei et al. (1996) was employed. In brief, samples were filtered through 0.22 μm pore filters and introduced using a 20 μL injection loop into a microbore column ODS-2 C_{18} (5 μm) 250 × 1.0 mm (MZ-Analytical) mount on a 1090 Series II HPLC system (Hewlett–Packard Co.) equipped with a Hitachi LaChrom L-7100 pump system and an HP 1046A UV detector. A linear gradient program of 10 mM KH_2PO_4 (A) and 10 mM KH_2PO_4 in 50% (v/v) methanol/water (B) (both at pH 4.5 adjusted with phosphoric acid) was used for the separation. The elution gradient (at 1 mL/min) was the following: 0–10% B in 15 min, 10–100% B in 15 min, hold at 100% B for 5 min, 100–4% B in 1 min, and a 20 min post run at 4% B. A detection wavelength of 292 nm that corresponds to a maximum in uric acid absorption spectra was employed. Peak identity was confirmed by comparison to the elution time of known uric acid standards. Quantification was performed through a calibration curve that correlated the concentration of the uric acid standards to the corresponding peak areas.

2.6. Uricase activity

Uric acid oxidase activity was determined in culture extracts following the rate of uric acid disappearance. Specifically, properly diluted extract aliquots (20 μL) were added in 980 μL of 80 μM uric acid solution (in 100 mM borate buffer, pH 8) and uric acid consumption was monitored at 292 nm in a Hitachi UV–Vis (U-1100) photometer equipped with a thermostated cuvette holder (at 40 °C). Reaction rates (mM min^{-1}) were calculated from the ΔA_{292}/min using an appropriate calibration curve for uric acid in the above buffer. A boiled sample (10 min, 100 °C) undergone the same procedure was always used as blank. One unit (U) of uricase activity is defined as the amount of enzyme required for the transformation of 1 μmole of uric acid to allantoin per minute at the above described conditions. The specific activity of uricase was calculated by dividing the enzyme concentration in the samples (mU/mL) with the total protein concentration (mg/mL) determined through the Bradford assay (Bio-Rad).

3. Results and discussion

3.1. Purine utilization in the Eurotiales. Gene knock-outs and relative growth phenotypes

The availability of a number of genomes of the genera *Aspergillus*, *Penicillium*, *Talaromyces*, *Monascus* and *Thermoascus*, allowed us to check the presence of all the enzymes of purine catabolism discussed in this article in different species of the Eurotiales. The phylogeny and functional tests of the purine transporters will be discussed separately, it is sufficient to say here that almost all members of the Eurotiomycetes sequenced have UapA/UapC and AzgA homologues (E. Krypotou, C. Scazzocchio and G. Diallinas, unpublished). The purine utilization pathway of *A. nidulans* together with cognate enzymes, transporters and corresponding genes is shown in Fig. 1A. The phenotypes of several mutations in each gene have been described in a number of publications and are summarized in Gournas et al. (2011). Null mutations, either total deletions and/or early chain termination mutations of *uapA*, *uapC*, *azgA*, *hxA uaZ*, *uaX*, *uaW*, *uaY* and *xanA*, were already available (for details see Table S1).

3.1.1. Hypoxanthine and xanthine conversion to uric acid

Xanthine dehydrogenase (Purine hydroxylase I, XDH, HxA) is present in all Aspergilli in the data bases in highly syntenic positions and is also present in all Eurotiomycetes species sequenced. In *A. nidulans* a paralogue has been characterized genetically and biochemically, purine hydroxylase II, which is physiologically a nicotinate hydroxylase, encoded by the *hxnS* gene (Scazzocchio et al., 1973; Lewis et al., 1978; Scazzocchio, 1980, 1994). This has now been formally identified as AN9178. The identification, regulation, phylogeny and linkage relationships of *hxnS* will be discussed separately (H. Hamari, R. Fernández-Martín, M. Flipphi, A. Cultrone, J. Kelly and C. Scazzocchio, unpublished). Not surprisingly, *hxB* encoding a MOCO sulphurase (Amrani et al., 2000, see Fig. 1A) necessary for the activity of both HxA and HxnS, is also universally present and shows a high degree of synteny, except in *A. nidulans*, *A. versicolor* and *A. sidowii*, where an inversion of neighbor genes compared with other Aspergilli is observed.

XanA (xanthine α-ketoglutarate dependent dioxygenase), is present in syntenic positions in the Aspergilli but absent from *A. fumigatus* (both strains available) and *N. fischeri*. This absence has been confirmed by BlastN and tBlastN (see Table S3). As it is present in *A. clavatus*, there seem to have been an episode of loss in *A. fumigatus*/*N. fischeri* clade. Among the Eurotiales it is absent also in *Thermoascus auratiancus*. Clear orthologues of XanA are present in all *Penicillium* and *Taleromyces* species. Interestingly, most species show additional paralogues, *P. canescences* showing as many as five paralogues. Residues involved in iron chelation (in XanA of *A. nidulans* R147, H149, H340) and typical of dioxygenases are almost always conserved in these paralogues, with some substitutions by polar residues which in principle could chelate Fe^{++} while α-ketoglutarate binding residues are less conserved, noticeably in the most divergent paralogues opening the possibility that these may use a different co-substrate. Asn358 (numbering as in *A. nidulans* XanA), involved in catalysis is highly conserved except in some of the most divergent paralogues, while substitution of the substrate binding residues predicts a different specificity for the more divergent paralogues (Fig. S2). The phenotype of the *xanA* deletion can only be detected in the background of mutations resulting in the loss of purine hydroxylase I activity, such as the *hxA*, *hxB* or *cnx* mutations (Cultrone et al., 2007; shown in Fig. 1C for a *xanA*Δ *hxA18* double mutant).

3.1.2. Urate conversion to allantoin

The genes encoding the three enzymes involved in the conversion of urate to allantoin, *uaZ*, *uaX* and *uaW* are conserved in syntenic positions in the Aspergilli. They are conserved in all Penicillia/Talaromyces species available, even if in some cases they are not recorded in the data bases. Interestingly, *A. brasiliensis*, *A. tubigensis* and *A. niger* also possess a second UaZ orthologue displaying an amino acid sequence identity of over 60% with the first one (Table S3). All UaZ homologues in Aspergilli carry predicted carboxy-terminal PTS1 sequences of the types (K/S)(A/P/S)KL, most frequent being KAKL. In addition, all UaX homologues carry conserved PTS2 sequences of the type – RLxLY(R/Q)x(H/Q)L – in the amino-terminal region.

3.1.3. Ureide metabolism: conventional and alternative pathways

The possible structural genes for allantoinase and allantoicase were defined earlier as *alX* and *aaX* genes respectively on the basis of growth tests (Darlington et al., 1965) and enzyme assays (Scazzocchio and Darlington, 1968). The *alX4* allele was characterized as a chain termination mutation on the basis of its suppressibility by *suaB111* (Roberts et al., 1979), which is a mutation in the anticodon of a glutamine tRNA (Espeso et al., 2005). *alX* has been tentatively identified with AN4603 (Hamari et al., 2009). The putative gene encoding allantoicase, AaX, was identified by BlastP, using the sequence of the *Saccharomyces cerevisiae* DAL2 (YIR029W) as probe. We constructed total loss-of-function mutations by complete deletions of ORFs for *alX* (AN4603) and *aaX* (AN3104) by standard reverse genetics approaches (see Section 2). The phenotypes of the newly constructed deletions are consistent with those previously described for classical genetic mutants (Fig. 1C; Darlington et al., 1965; Scazzocchio and Darlington, 1968). The identity of the *alX* and *aaX* genes has been further confirmed by sequencing the previously genetically and enzymatically characterized mutations *alX4* and *aaX1* (Scazzocchio and Darlington, 1968). *alX4* is a CAG to TAG transition in codon 409 (Q409Amber, also sequenced by Liu et al. (2014)). *aaX1* is GGG to TGG transversion in codon 196, resulting in a G196W substitution, that is predicted to localize on a very short β-strand leading to the flexible linker region connecting the two β-sandwich allantoicase repeats, when modeled on the crystal structure of the *S. cerevisiae* allantoicase (YIR029W; PDB: 1059; Fig. S3).

A. sydowii and *A. versicolor* appear to possess a second almost identical allantoinase orthologue, probably as a result of a recent duplication; however, in many Aspergilli and other members of the Eurotiales at least one other paralogue of *alX* exists (Fig. S4A). This paralogue(s) cannot have any role in allantoin utilization during vegetative growth as a chain termination mutant, *alX4*, and the newly constructed *alX* deletion are completely non-leaky for the utilization of allantoin and its precursors (see Fig. 1C). Fig. S4B compares the two paralogues present in *A. nidulans* with AlX. All active site residues, as deduced from the structure of the allantoinase of *E. coli* (Kim et al., 2009) are conserved in AlX and its *S. cerevisiæ* orthologue Dal1p, while the residues which contact specifically allantoin in the structure are not conserved in the two paralogues. The paralogue denoted as AN8418 is in an apparent gene cluster in chromosome III with another putative amide hydrolase encoding gene, AN8417 (comprising two PFAM domains, carbon–nitrogen amino hydrolase, PF00795 and Asp/Glu/Hydantoin racemase, PF001177), transcribed divergently, while AN8416 encodes FurE (Hamari et al., 2009), a paralogue of the specific allantoin transporter FurA. It is highly probable that the three genes are co-involved in the utilization/degradation of an unknown metabolite.

Ramazzina et al. (2008) have established that in a number of organisms, both eukaryote and prokaryote, the hydrolysis of allantoin to allantoic acid is catalyzed by a completely different enzyme (called PuuE in *Pseudomonas fluorescens*, usually annotated as a polysaccharide deacetylase). In *A. nidulans* the protein encoded by AN9327 looks like a perfect orthologue of the *P. fluorescens* PuuE, all active site residues being conserved. A second paralogue, AN3354, lacks a critical Glu residue involved in the binding of allantoin, (E36 in the PuuE enzyme, Ramazzina et al., 2008) and may accept a different substrate (see Fig. S5). Interestingly, AN3354, separated from it by a gene encoding a protein of unknown function, is close to the uracil/allantoin-like transporter FurC, whereas, AN9327 neighboring gene, AN11211, is *furF*, encoding another member of the Fur-transporter family (Hamari et al., 2009). The following gene, AN11219, only 189 base pairs away encodes a putative amidase (PFAM domain PFO1425), a situation similar to that described above for AN8418. Possible homologues are present in *A. sydowii* and *A. versicolor* but not in other Aspergilli. The functional significance and phylogeny of the *A. nidulans* homologues of PuuE are under investigation and will be published separately (S. Amillis and C. Scazzocchio, unpublished).

No orthologue of AN3104 (*aaX*) is present in *A. clavatus A. flavus*, *A. oryzæ*, *A. terreus* and *A. versicolor*. Among other members of the Eurotiomycetes, it is absent from *Gymnascella auriantica*, most of the Penicillia (present in *P. digitatum*, *P. expansum*, *T. marmeffei*, *T. stipitatus* and *Thermoascus expansum*, absent in all others including *P. chrysogenum*). However, at least several of the organisms mentioned above utilize purines as nitrogen source (see Fig. 1B), thus they must be able to degrade allantoic acid. An allantoicase activity, measured by glyoxylic acid production from potassium allantoate was also shown in crude extracts of an unspecified strain of *P. chrysogenum* (Allam and Elzainy, 1969). These results imply that an alternative allantoicase, enzyme or pathway, not homologous to AN3104 (*aaX*), must be present in some members of Eurotiomycetes and probably in other fungi. A very recent article describes precisely this alternative enzyme, an ureidoglycine hydrolase (UGLYAH2), which is also able to accept allantoic acid as a substrate, and noted that this alternative pathway is present in *A. oryzae* and *P. chrysogenum* (Puggioni et al., 2014). Putative UGLYAH2 orthologues are present in precisely those species of the Eurotiomycetes which lack allantoicase, with only one species, *A. sydowii*, having both an orthologue of AaX and UGLYAH2. The similarity with bacterial UGLYAH2s is striking, with about 70% identity with the characterized protein of *Pseudomonas aeruginosa* (Fig. S6A), reaching 91% identity with a orthologue of *Ochrobactrum intermedium*, higher than that found between the enzymatically characterized enzyme of *Agrobacterium tumefaciens* and the structurally characterized enzyme of *P. aeruginosa* (64%, Puggioni et al., 2014). All metal and substrate binding residues are strictly conserved (Fig. S6). This strongly suggests a recent horizontal transmission from bacteria to an ancestor of the Eurotiomycetes. To gain further information on this hypothetical event we searched all the available fungal genomes in both the NCBI and JGI databases. We found very close orthologues (besides the Eurotiomycetes mentioned above; identities with the protein of *A. oryzae* 80%) only in *Metarhizium anisopliae*, *M. acridum* (Sordariomycetes, Hypocreales), *Pseudogymoascus destructans* (Leotiomycetes), *Fusarium oxysporum*, *F. fujikuroi* and *F. gramminearum* (Sordariomycetes, Hypocreales) and *Claviceps purpurea* (Sordariomycetes, Hypocreales). Of these, only the *Fusarium* species have both a classical allantoicase and UGLYAH2. It may be relevant that none of the cognate genes, either in these species or in the Eurotiomycetes mentioned above, are interrupted by introns. As genes encoding the UGLYAH are found in a scattered fashion in three different orders within the Pezizomycotina, it is a moot point whether more than one horizontal transfer event was involved. Interestingly, the UGLYAH homologues of *A. terreus*, *A. versicolor* and *A. sydowii* are also predicted to have a low score PTS1 sequence of the type RS(R/K)I. The same article describes an enzyme, allantoate aminohydrolase

(AAH), which catalyses the hydrolysis of allantoate to ureidoglycine. This enzyme is an obligatory first metabolic step in organisms (such as *Arabidopsis thaliana*) where the UGLYAH is strictly specific for ureidoglycine and unable to hydrolyze allantoate. It occurs also in some organisms where UGLYAH2 is extant such as *A. oryzae* (Puggioni et al., 2014). Using the *A. oryzae* enzyme sequence as *in silico* probe we detected possible homologues (including several paralogues in the same genome) in all members of the Eurotiomycetes. As, differently from UGLYAH2, no structural information is available for AAH, is not possible to have any inkling as to the substrate specificity of these paralogues.

Ureidoglycolate lyase (also called hydrolase, nomenclature as in Percudani et al., 2013) converts ureidoglycolate, originating from the hydrolysis of allantoic acid to urea and glyoxylate. Mutations in the cognate gene could not be isolated by Darlington et al. (1965) as one mole of urea is produced by the previous step of the pathway (see Fig. 1A), and thus an eventual mutation would not prevent the growth on purines as nitrogen sources. The enzyme activity is present in *A. nidulans* crude extracts (Scazzocchio and Darlington, 1968). A putative gene encoding this enzyme could be unambiguously identified by similarity with DAL3 (YIR032C) from *S. cerevisiæ* as AN1480. All putative metal binding residues of the active site, as deduced by the structure of the *E. coli* enzyme AllA (Raymond et al., 2005) are absolutely conserved in DAL3 and in the ORF of AN1480 (corresponding to D128, H130, Q135 and H204 in the AN1480 sequence; not shown). The enzyme has been reported to be localized in the peroxisome in *Candida tropicalis* (Takada and Tsukiji, 1987). A carboxy-terminus PTS1 sequence TAKL is present in this species and the orthologues of other *Candida* species but not in DAL3 of *S. cerevisiæ*. The carboxy terminus of AN1480 is QAKL, predicting a peroxisomal localization, which is conserved throughout the Eurotiales, while *P. expansum* has a second paralogue which does not have a PTS1. Putative orthologues are present in all Eurotiales, even though in *A. flavus* and *A. terreus* they are not recorded in the protein databases. In this work, a complete deletion of the AN1480 (named *uglA*) ORF was constructed (see Section 2). A leaky mutant phenotype is visible in a *uglA*Δ strain, most noticeably on allantoin as nitrogen source, the latter possibly due to the accumulation, from its precursor, allantoic acid, which is highly toxic to the cell (Darlington and Scazzocchio, 1968).

3.2. Subcellular localization of enzymes of the purine utilization pathway

gfp-tagged versions of all the genes encoding the enzymes studied were constructed by standard reverse genetics resulting in *in locus* substitutions of the wild type gene with the *gfp* tagged version driven by its physiological promoter (for each particular substitution see Supplementary Materials and Methods). Fully functional C-terminal GFP-versions of the UapA, AzgA and UapC transporters were already available and their localization has been described (Pantazopoulou et al., 2007 and refs therein). The *gfp*-ORF was linked N-terminally with the gene of interest. For *aaX*, two different N-terminal GFP fusions were constructed, due to the existence of two in-frame putative translation initiation codons and the protein length discrepancy observed among comparing homologues proteins in other Aspergilli (see below). For *hxA*, *uaZ* and *xanA*, *gfp* C-terminal fusions were also constructed. As shown in Fig. 1C, N-terminally tagged GFP versions of enzymes, including both *aaX* fusions (shown only for AaX^{ATG2}; see below), have growth phenotypes identical to the *wt*. An exception is UglA, where the N-terminally tagged GFP version results in a leaky mutant growth phenotype. C-terminally tagged GFP versions result in leaky mutant (UaZ-GFP) or even null (HxA-GFP, XanA-GFP) mutant phenotypes (not shown). For HxA, possibly the C-terminal fusion interferes with enzyme dimerization. HxA and its paralogue HxnS are active as dimers and the stringent specificity of dimerization is shown by the fact that heterodimers were never detected (Lewis and Scazzocchio, 1977; Lewis et al., 1978). The structure of the strictly conserved bovine orthologue of HxA shows that the dimerization domain is in the C-terminus of the protein (Enroth et al., 2000). For UaZ, the partial functionality of the C-terminally tagged enzyme is compatible with the fact that UaZ has a canonical peroxisomal targeting signal 1 (PTS1) at its C-terminus (see also later), which is probably masked by the GFP. Further work was carried out with the N-terminally tagged fusions.

Fig. 2A shows an epi-fluorescence analysis of young growing mycelia from strains expressing the functional N-terminally GFP-tagged enzymes mentioned above, grown under optimally inducing conditions (see Section 2). When inducer was not added, the expression of most enzymes was very low (at the limit of detection), but enzyme localization was identical to the one obtained after uric acid induction (not shown). For GFP-UglA, addition of uric acid did not affect protein expression levels, a fact which is in agreement with previous work, which showed the expression of the enzyme to be constitutive (Scazzocchio and Darlington, 1968).

The expression level of the annotated *aaX* gene tagged at the first putative ATG (AaX^{ATG1}; ChrVI_A_nidulans_FGSC_A4:1813244-1814472), was at the limit of detection, displaying a weak diffuse distribution (not shown), whereas the *gfp*-tagged version starting at nt +135 (second putative ATG) showed a much stronger expression signal (Fig. 2A). HxA, AlX, AaX, UaW and XanA were diffusedly localized in the cytoplasm and excluded from nuclei and/or vacuoles, whereas UaZ, UaX and UglA formed distinct cytoplasmic foci, which do not overlap with structures observed by terminal endocytic staining with FM4-64. The number of these foci, which we subsequently showed to correspond to peroxisomes (Fig. 2B and C; see below), was estimated to be 4–6 in each hyphal compartment separated by septa, a picture similar to the one describing the peroxisomal localization of *A. nidulans*, *A. fumigatus* and *Neurospora* siderophore biosynthetic enzymes (Gründlinger et al., 2013).

Peroxisomal localization of UaZ, UaX and UglA is in agreement with the presence of canonical peroxisomal targeting signals (PTS) on these enzymes. UaZ and UglA contain the sequence AKL at their extreme C-terminus, which is compatible with a canonical PTS1 (A/SKL motif). This signal is conserved in all ascomycete UaZ homologues and also in most *Aspergillus* UglA homologues (P/A/S/G-K-L). The N-terminus of UaX contains the sequence ^{20}RLNLYQNHL^{28}, conserved also in all other Aspergilli, which is compatible with canonical PTS2 motifs [(R/K)(L/V/I/Q)xxxxx(H/Q)(L/A/F/I), (Petriv et al., 2004, shown also previously to be operational in *A. nidulans*, Hynes et al., 2008). It is noticeable that such a motif occurs also in the biochemically and crystalographically characterized orthologue from *Danio rerio* and in general in metazoan homologues (Ramazzina et al., 2006; Zanotti et al., 2006).

Direct evidence that the GFP-UaZ-labeled foci are indeed peroxisomes came from the observation that the same pattern of labeling is obtained with mRFP carrying in its C-tail the putative peroxisomal localization signal of UaZ, Ala-Lys-Leu (Fig. 2B). To further show that foci labeled with GFP-UaZ, GFP-UaX and GFP-UglA, correspond to peroxisomes, *pexE*Δ or *pexG14* alleles were combined in strains expressing GFP-tagged enzyme versions. *pexE* and *pexG* are the genes encoding the PTS1 and PTS2 receptors necessary for peroxisomal protein targeting (Hynes et al., 2008) respectively. We note that while *pexE*Δ and *pexG14* affect the growth of *A. nidulans* (Hynes et al., 2008), no specific additional effect on the utilization of purines as nitrogen sources was detected (not shown).

Fig. 2D shows that in the relevant *pex* genetic backgrounds GFP-UaZ, GFP-UaX and GFP-UglA are localized diffusedly in the cytoplasm, rather than forming the characteristic peroxisomal foci.

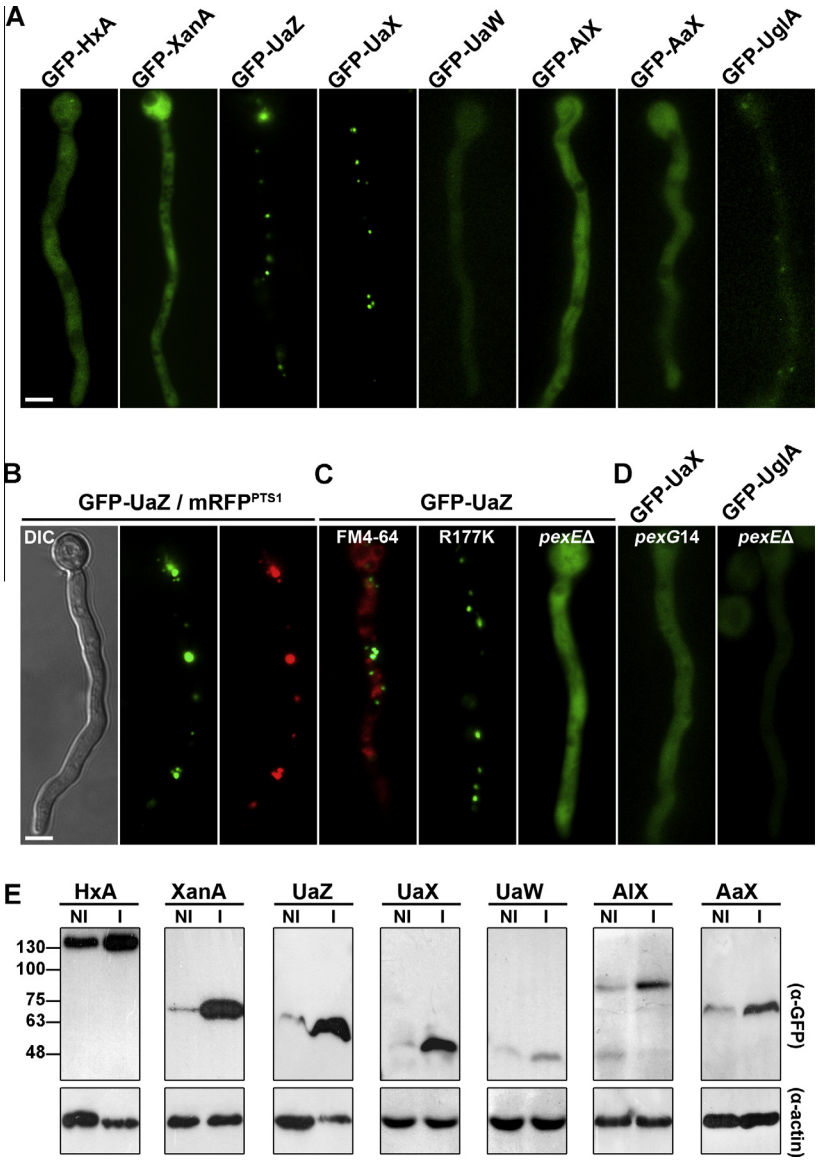

Fig. 2. Localization and expression of purine catabolic enzymes in mycelia. (A) Microscopic analysis of functional N-terminal GFP-tagged versions of HxA, XanA, UaZ, UaX, UaW, AlX, AaX and UglA grown on MM supplemented with $NaNO_3$ as nitrogen source and induced with uric acid for 14–16 h at 25 °C. Due to a weak signal, GFP-UaW and GFP-UglA are shown overexposed. (B) GFP-UaZ co-localization with mRFP fused to the UaZ C-terminal putative PTS1 peroxisomal signal sequence. (C) Left panel: GFP-UaZ expression under the same conditions as in (A) co-stained with FM4-64 at terminal endocytic stages (40 min). Middle panel: GFP-UaZ peroxisomal localization is not altered in a strain carrying the total loss-of-function mutation R177K. Right panel: GFP-UaZ localization in the cytoplasm in a *pexE*Δ mutant. (D) GFP-UaX and GFP-UglA localization in the cytoplasm in a *pexG14 or pexE*Δ mutant respectively. Scale bar: 5 μm. (E) Western blot analysis of total protein extracts of strains carrying N-terminal GFP-tagged versions of HxA, XanA, UaZ, UaX, UaW, AlX and AaX, grown on MM supplemented with nitrate (non-induced; NI) or on in the simultaneous presence of uric acid (induced; I). Equal loading (50 μg) is monitored by a monoclonal α-actin antibody. (For interpretation of the references to colour in this figure legend, the reader is referred to the web version of this article.)

For UaZ, we also show that the localization of an inactive version of the enzyme, due to a specific substitution of a crucial for enzyme activity Arg residue (Arg177Lys; Ito et al., 1991) in its active site, and resulting in inability of the strain carrying it to utilize uric acid (not shown), is identical to the one obtained with wild-type GFP-UaZ (Fig. 2C).

Fig. 2E shows a western blot analysis of GFP-tagged enzymes using anti-GFP antibodies. Total proteins were isolated from young mycelia under non-inducing or uric acid-inducing conditions. With the exception of GFP-UglA that could not be detected by western blotting and of GFP-AaX^{ATG1} that was again at the limit of detection (not shown), induction by uric acid led to significant increase in the steady state levels of the enzymes tested. All N-terminally GFP-tagged enzymes showed intact bands at the expected molecular weight of the corresponding chimeric construct. This result confirms that the localization of all enzymes observed microscopically corresponds to the *in vivo* localization of the untagged enzymes, and it is not a result of the tagged enzyme degradation. Previous *in vitro* work suggesting proteolysis of XanA is most probably an artefact of the purification procedure, with no significance for enzyme localization (Montero-Morán et al., 2007).

3.3. Expression of purine utilization enzymes and transporters in asexual differentiated cells and phenotypes associated with the *uaZ*$^{-}$-dependent uric acid accumulation

The subcellular expression and localization of GFP-tagged enzymes were further examined in the differentiated asexual compartments of *A. nidulans* (conidiophores, vesicles, metulae, phialidiae, and conidiospores). All enzymes were well expressed and

showed a similar subcellular localization as those detected in germlings and vegetative hyphae. A more pronounced signal was obtained at the level of metullae for the cytoplasmically localized enzymes, whereas peroxisomal enzymes were expressed mostly in the conidiospores (Fig. 3). The activity of uricase (mU/mg protein) in conidiospores was also confirmed by enzymatic assays (see insert in Fig. 3). UapA and AzgA transporter expression and localization in the asexual compartments of *A. nidulans* have been previously examined (Pantazopoulou et al., 2007; Diallinas, 2008). Interestingly, while AzgA-GFP is practically not expressed, UapA-GFP gave a strong signal at the periphery of the metulae and to a lesser extent in the phialidiae, while it was absent in the conidiospores. Here we show the localization of UapA is also shared with its paralogue UapC (Fig. 3), suggesting that only those purine transporters specific for uric acid and xanthine seem to have a function in the compartments of the conidiophore of this fungus.

To further investigate the role of UapA and UapC in the metullae and phialidiae, we measured metabolic uric acid levels in vegetative mycelia or conidiospores grown under non-repressing nitrogen source conditions (urea) in isogenic wild-type (*wt*), *uapAΔ uapCΔ*, *uaZ14* and *uaZ14 uapAΔ uapCΔ* strains (Table 1). Wild-type and *uapAΔ uapCΔ* cells showed very low, but measurable, amounts of uric acid in extracts of mycelia (~4–5 nmoles/mg protein) and conidiospores (~1 nmole/mg protein). The *uaZ14* mutant showed dramatically increased levels of uric acid (73 and 119 nmoles/mg protein, respectively), which is in agreement with the absence of urate oxidase as was demonstrated by Darlington and Scazzocchio (1968). Interestingly, in the *uaZ14 uapAΔ uapCΔ* mutant, high levels of uric acid (59 nmoles/mg protein) were observed in mycelia, but were dramatically reduced in conidiospores (~3 nmoles/mg protein). This implies that high levels of uric acid produced through incomplete purine breakdown in mycelia are actively transported to the conidiospores through the activity of UapA and UapC expressed in metullae and phialidiae. Thus these, fungal transporters have a dual role, supplying mycelia with compounds that can be used as nitrogen sources but also re-distributing metabolites in differentiated cells of the conidial apparatus. Our observations suggest an additional level of developmental regulation of the expression of the genes encoding some of the transporters and enzymes of the purine utilization pathway.

Uric acid can serve *in vivo* both as an anti-oxidant or a pro-oxidant depending on its concentration and biochemical environment. The unexpected finding that uric acid accumulates in conidiospores, most probably transported by UapA and UapC present in the conidiophore, led us to investigate whether uric acid accumulation in conidiospores has a role other than serving as a nitrogen source. To this aim, we compared isogenic wild-type and *uaZ* null mutant phenotypes in conditions of oxidative stress and UV radiation. Highlights of our results are summarized in Fig. 4A–E. Mutants in *uaZ* were found not to be associated with obvious gross growth impairment (25–37 °C, for 2–4 days) when compared with strains grown on nitrogen sources other than purines under standard conditions (not shown). However, we did detect phenotypic differences between *uaZ* null mutants and isogenic *uaZ*$^{+}$ control strains after prolonged growth in CM or MM. Firstly, prolonged growth of *uaZ* null mutants, in both solid and liquid media, was not associated with a brownish coloration observed for isogenic wild-type strains (Fig. 4A). The biochemical basis of this coloration is not known, but seems to be associated with colony ageing. A similar protection from the appearance of brownish coloration has also been observed when we added ascorbic acid in the medium (not shown), suggesting that the protective effect of uric acid might also be due to its anti-oxidant properties. Secondly, the density of conidiophores in *uaZ* null mutants, as shown for *uaZ14* in a stereoscope, and the estimated total number of conidiospores per cm^2, was lower than that of the control strains

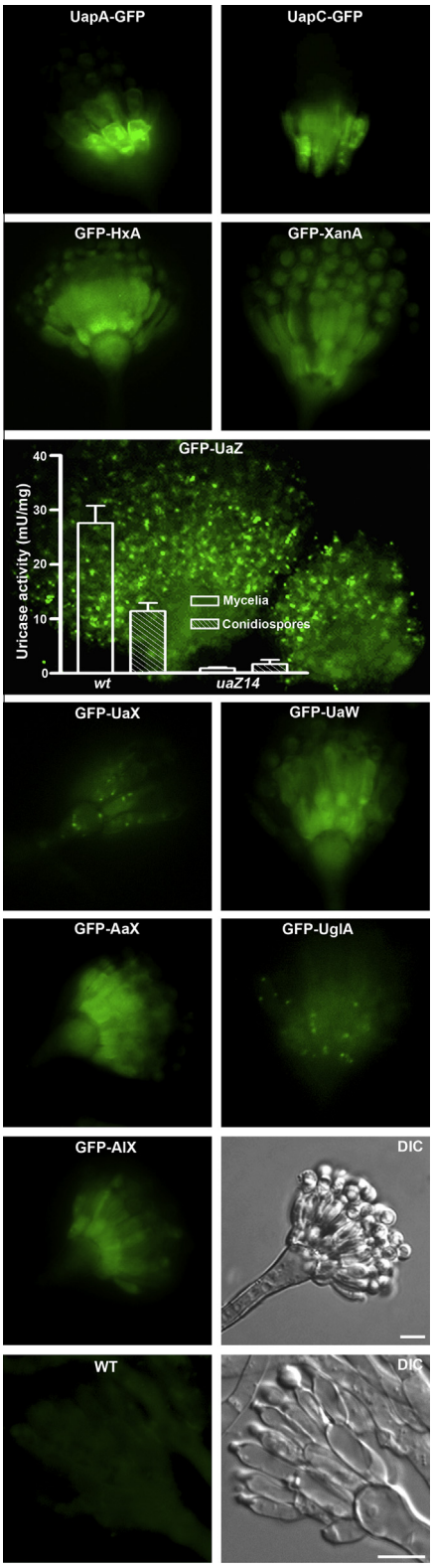

Fig. 3. Expression of enzymes of the purine catabolism during asexual differentiation. Conidiophores of strains expressing GFP-tagged UapA, UapC, HxA, XanA, UaZ, UaX, UaW, AlX, AaX and UglA grown on MM supplemented with nitrate as sole nitrogen source and induced with uric acid for 6 days at 25 °C. All conidiophores are at a similar growth stage as shown for AlX, except in the case of UaZ (middle panel) where a more developed conidiophore is also shown. The bottom panel shows a control of conidiophore auto-fluorescence detected in a *wt* strain (WT). Scale bar: 5 μm. Uricase (UaZ) specific activities (mU/mg protein) in conidiospores and mycelia in *wt* and a *uaZ14* loss-of-function mutant are shown embedded in this middle panel (see Section 2).

Table 1
Estimation of uric acid levels by HPLC. Uric acid levels (nmoles) per mg protein in mycelia or conidiospore extracts in *wt* and mutant strains altered in respect to the catabolism and/or the uptake of UA (*uaZ14*, *uapAΔ uapCΔ*, *uaZ14 uapAΔ uapCΔ*). Uric acid accumulation in conidiospores is dependent on uric acid transporter (UapA/UapC) expression. Data represent the average ± SD of triplicate experiments.

	wt	*uapAΔ uapCΔ*	*uaZ14*	*uapAΔ uapCΔ uaZ14*
Mycelia	3.46 ± 0.46	5.12 ± 1.89	73.19 ± 7.18	58.83 ± 7.07
Conidiospores	1.03 ± 0.32	0.93 ± 0.19	119.30 ± 21.44	3.32 ± 0.98

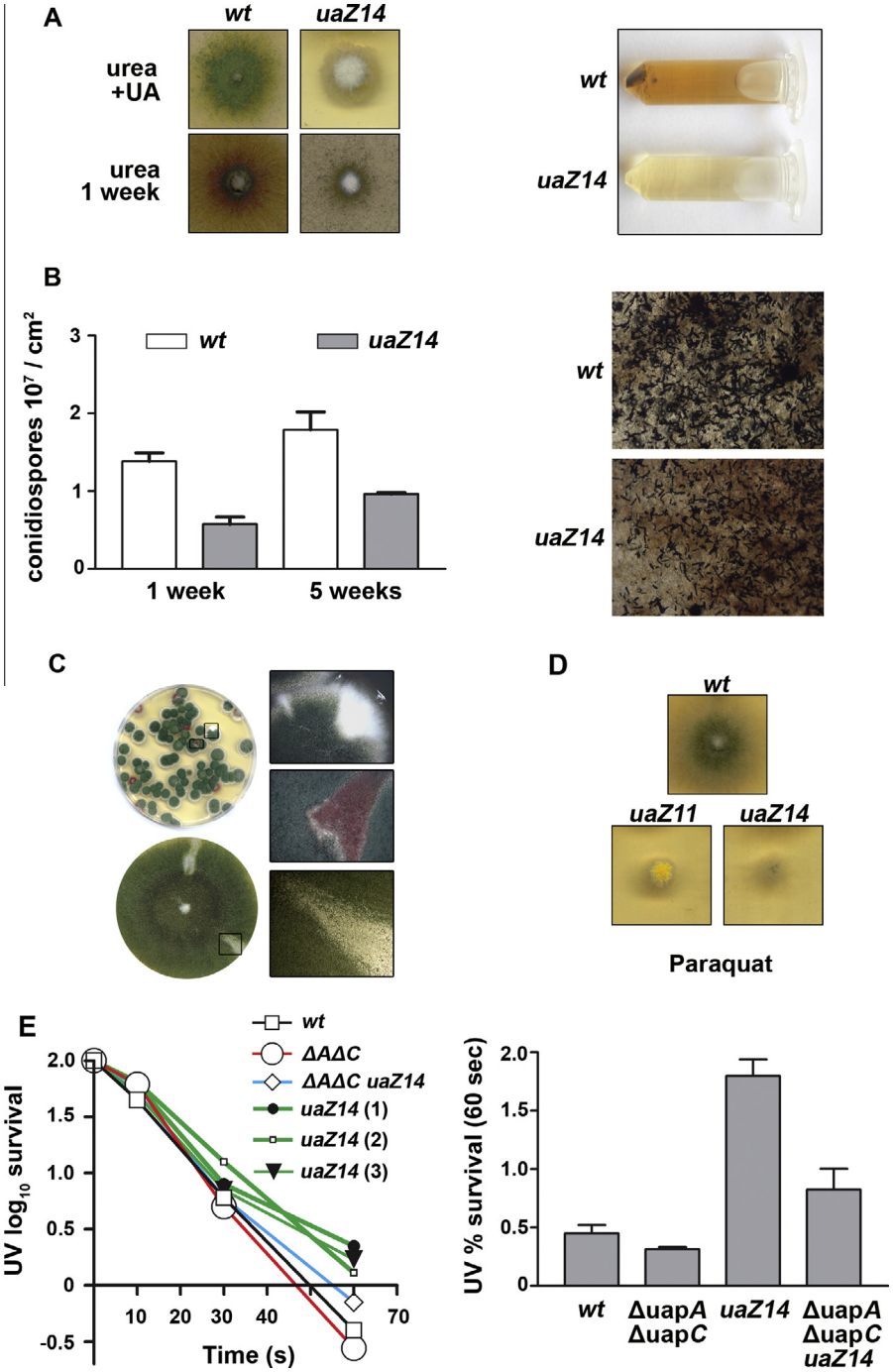

Fig. 4. Phenotypes related to uric acid accumulation due to loss-of-function mutations in *uaZ*. (A) Phenotypic differences between isogenic *wt* and *uaZ* null mutants after prolonged growth in both solid and liquid MM media at 37 °C. Mutant *uaZ14* is sensitive to the presence of 1 mM uric acid (UA) in the medium, but does not show a brownish coloration after prolonged growth. The right panel shows that the brownish coloration in the *wt* is associated with the supernatant of the culture. (B) Conidiospore production in *uaZ14* is lower than in an isogenic *wt*. The right panel shows a stereoscopic view of solid cultures of the two strains. (C) Mutant *uaZ14* exhibits increased appearance of spontaneous morphological sectors. (D) Hypersensitivity of mutants *uaZ11* and *uaZ14* in the presence of paraquat. (E) Resistance of *wt* and mutants to UV exposure. Notice the increased relative resistance of the three independent strains carrying the *uaZ14* at 60 s of UV exposure. (For interpretation of the references to colour in this figure legend, the reader is referred to the web version of this article.)

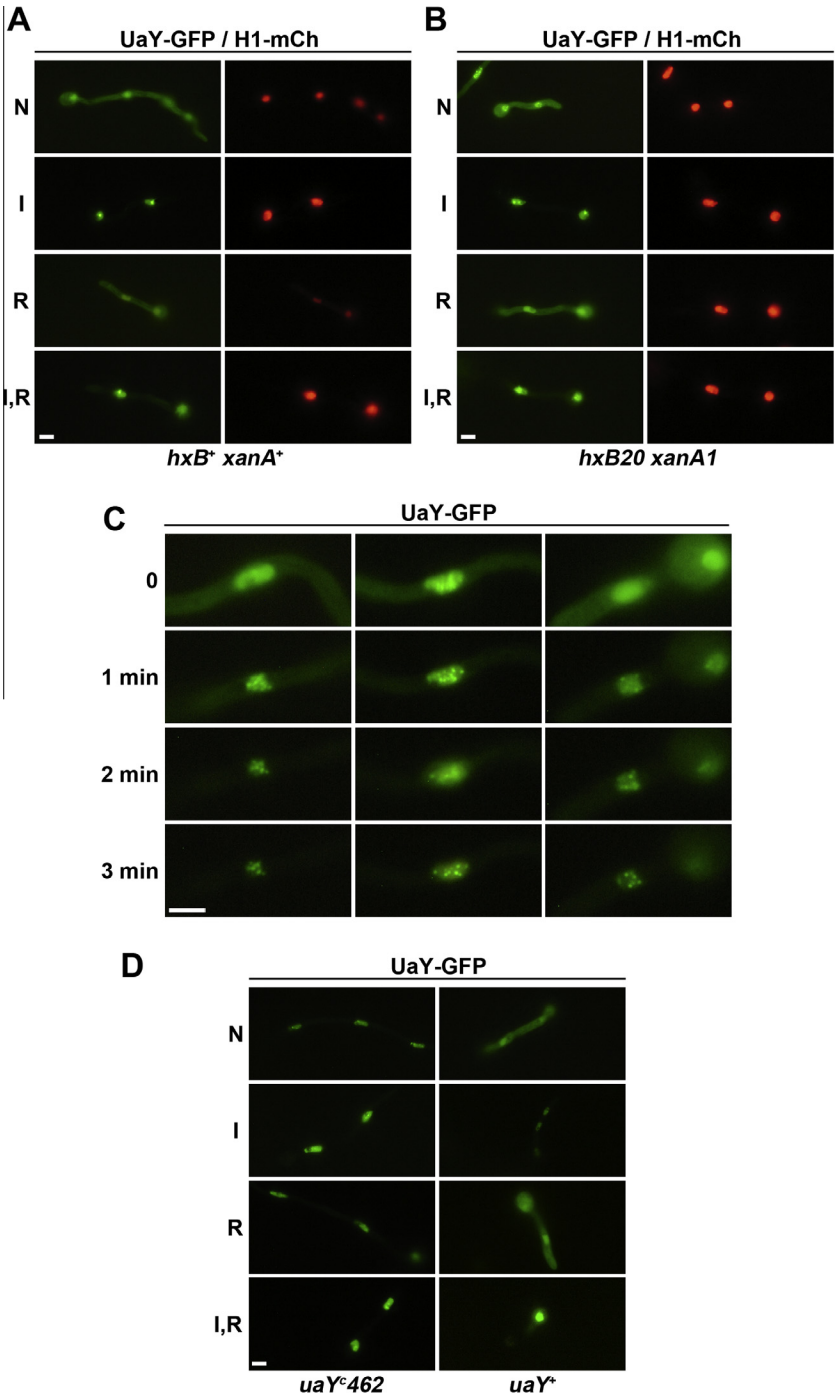

Fig. 5. Subcellular localization of the UaY transcription factor. Panels and (A) and (B). Subcellular localization of UaY-GFP (green), driven by the *gpdA* promoter and *hhoA-mCh* (tagged histone H1) in a *hxB*$^+$ *xanA*$^+$ and *hxB20 xanA1* genetic backgrounds respectively. Growth conditions are described in Section 2. N, Non-inducing conditions (16 h urea); I, inducing conditions (addition of uric acid for the last 2 h); R, repressing conditions (addition of ammonium for the last hour); I,R induction followed by repression. (C) Mycelia of a strain carrying the *gpdA-uaY-gfp* construction were grown for 16 h on urea. After the picture at time 0 was taken, 5 μL of a solution of 500 μM uric acid were introduced by capillarity between slide and cover slide, and pictures were taken every minute as indicated. We show three independent experiments. (D) Subcellular localization of UaY^{c}462-GFP. Strains carrying either the *uaY-gfp* fusion (*uaY*$^+$) or the *uaY*^{c}*462-gfp* (*uaY*^{c}*462*), both under the control of the *prnD* promoter, were grown for 17 h at 25 °C in the presence of fructose as sole carbon source and urea as sole nitrogen source. At 14 h proline was added to induce expression of the fusions, this does not induce the purine catabolic pathway. Non-inducing, inducing, repressing and repressing-inducing conditions were the same as in (A–B). Scale bar: 5 μm. (For interpretation of the references to colour in this figure legend, the reader is referred to the web version of this article.)

(Fig. 4B). Thirdly, an increased appearance of spontaneous morphological sectors (fluffy or aconidial) is significantly more frequent in *uaZ* null mutants than in control strains (Fig. 4C). A number of *uaZ*$^-$ progeny of a *uaZ*$^+$/*uaZ14* cross also showed spontaneously appearing morphologically altered sectors (not shown). A very recent article reports the appearance of morphological sectors after prolonged growth *A. nidulans* in the presence of H_2O_2, some of the sectors shown being uncannily similar to those reported in Fig. 4C (Li et al., 2014). *uaZ* null mutants (*uaZ14*, *uaZ11*; see Table S1 and Section 2) are hypersensitive to paraquat, a strong oxidation agent (Fig. 4D), suggesting that uric acid can also act as a pro-oxidant in the presence of other reactive oxygen species.

Finally, as shown in Fig. 4E, accumulation of uric acid in the conidiospores of three different *uaZ14* strains derived from a *uaZ*$^{+}$/*uaZ14* genetic cross, results in an increased resistance to UV radiation which is particularly detectable at 60 s of UV-exposure. This protective effect is UapA/UapC-dependent, confirming that uric acid is translocated from mycelia to the conidiospores through the metullae and phialidiae in a carrier-dependent manner.

3.4. Nuclear-cytoplasmic shuffling of the UaY pathway-specific purine utilization transcription factor

UaY, the specific transcription factor of the *A. nidulans* purine utilization pathway is universally conserved in the Pezizomycotina (our unpublished observations). However, it has been studied in detail only in *A. nidulans* (Suárez et al., 1995; Cecchetto et al., 2012 and refs therein) and functionally identified in *Neurospora crassa* (Liu and Marzluf, 2004).

In this section we analyze the nucleo-cytoplasmic shuttle of UaY in response to induction by uric acid and repression by ammonium, which both signal gene expression in the purine utilization pathway (Scazzocchio and Darlington, 1968; Gournas et al., 2011, and refs therein). To this aim we constructed strains carrying carboxy-terminus *uaY-gfp* fusions driven either by the weak, physiological, *uaY* promoter or the strong constitutive *gpdA* promoter. In both cases the fusions were inserted *in trans* of a loss of function *uaY205* mutation (see Section 2). Fig. S7 shows that both constructions complement the *uaY205* mutation, including in strains carrying only one copy of the *uaY-gfp* fusion. The *gpdA-uaY-gfp* fusion, inserted at the *gpdA* locus in singly copy, results in 40–70 folds over-expression at the level of *uaY* transcription (not shown), which accounts for the growth on 6-methoxypurine, an analogue, which is not a nitrogen source for the *wt*, but can be utilized by *uaY* constitutive mutants (Suárez et al., 1991; Oestreicher and Scazzocchio, 1995). Transformants obtained by introducing one copy of *uaY-gfp* while complementing the *uaY205* mutation, did not show a fluorescent signal, while a strain carrying three copies of *uaY-gfp* showed a signal just above the level of detection (Fig. S8). A similar problem, where a construction driven with the physiological promoter did not result in a fluorescent signal, occurred also with the NirA transcription factor (Berger et al., 2006), which as UaY (Cove, 1969; Scazzocchio et al., 1982), is produced in strictly limiting concentrations, the latter being consistent with different experimental data discussed by Scazzocchio (1994). The *uaY-gfp* and *gpdAp-uaY-gfp* constructs behaved qualitatively identically. Under non-induced and repressed conditions, fluorescence is seen in the cytoplasm and the nuclei. Induction results in complete nuclear localization, while induction followed by ammonium repression results in only limited shuffling to the cytoplasm of the UaY-GFP molecules (Fig. S8).

In order to study more accurately the nucleo-cytoplasmic shuffling of UaY-GFP, the *gpd-uaY-gfp* construct was crossed into a strain carrying *hhoA-mCh*, which permits to identify nuclei by the red fluorescence of the H1 histone (Etxebeste et al., 2009). Fig. S9A shows that the presence of the tagged histone H1 does not interfere with the nuclear distribution of UaY-GFP. Results with the double labeled strain are shown in Figs. 5A and S8, which confirm completely the pattern of re-shuffling described above. The constitutive but limited presence of UaY in the nucleus is consistent with the dependence on UaY of the basal transcription levels of several purine utilization structural genes in the absence of inducer (Oestreicher and Scazzocchio, 1995, 2009; Cecchetto et al., 2012). Overexpression is unlikely to explain the presence of UaY-GFP in both the nuclei and the cytoplasm under non-induced conditions, as this pattern is seen also in the strain carrying three copies of *uaY-gfp* (Fig. S8D) at the limit of fluorescence detection. Nuclear localization upon induction is extremely rapid, been complete after 3–4 min of induction (Fig. 5C). The very limited extent of the reshuffling to the cytoplasm upon repression points to inducer exclusion in response of the presence of ammonium, rather than to an effect of ammonium on the UaY protein or a putative UaY/AreA complex (for a discussion of a similar effect on NirA see Berger et al., 2006; Bernreiter et al., 2007). This latter effect is consistent with the rapid internalization to endosomes of the UapA and UapC transporters (Valdez-Taubas et al., 2004; Pantazopoulou et al., 2007; Gournas et al., 2010; Karachaliou et al., 2013).

In a strain carrying both the *gpdAp-uaY-gfp* construction and mutations that prevent completely the conversion of intracellular purines to uric acid (*hxB20 xanA1*, Sealy-Lewis et al., 1978), the physiological co-activator of UaY, the pattern of UaY-GFP distribution remains unchanged (Figs. 5B, S8 and S9). Thus the presence of UaY-GFP in the nuclei under non-induced conditions is not due to low, intracellular, concentrations of uric acid.

The allele *uaY*^{c}*462* (S222L) results in constitutivity, hyper-inducibility and partial derepression of genes subject to UaY control (Oestreicher and Scazzocchio, 1995). When we attempted to introduce into *A. nidulans* a construction where the *uaY*^{c}*462-gfp* fusion is driven by the *gpdA* promoter, we only obtained transformants showing gross rearrangements of the input sequences or gene conversions at the recipient *uaY205* locus (see Section 2) which implies that the overexpression of *uaY*^{c}*462* is toxic to the cell. This is consistent with "squelching", an effect where the overexpression of one transcription factor impedes the expression of unrelated genes, by sequestering common components of the transcriptional machinery (Gill and Ptashne, 1988; Tavernarakis and Thireos, 1995). We thus drove the expression of both *uaY-gfp* and *uaY*^{c}*462-gfp* with the *prnD* promoter, inducible by proline (Gómez et al., 2002, 2003, see Supplementary Materials and Methods). The *prnDp-uaY*^{c}*462-gfp* strains are not able to grow in the presence of 5 mM proline, which confirms the toxicity of *uaY*^{c}*462* overexpression. To analyze the nuclear/cytosolic distribution of the *uaY*^{c}*462-gfp* construction, this strain was grown on urea, pre-induced with proline for 4 h before carrying on the observations reported in Fig. 5D. We thus determined that the *uaY*^{c}*462* mutation results in complete nuclear localization of the fusion protein under all conditions tested. The fact that UaY^{c}462 responds to uric acid induction (Oestreicher and Scazzocchio, 1995) implies that, as demonstrated also for the NirA transcription factor, constitutive localization to the nuclei is a necessary but not sufficient condition to achieve fully constitutive expression of the cognate regulated genes (Bernreiter et al., 2007).

Promoting nuclear localization is one of the possible mechanisms by which an inducer signal could affect the activity of a transcription factor. In *A. nidulans*, AlcR and PrnA are exclusively nuclear under both non-induced and induced conditions, and for the latter it has been shown that induction results in binding to specific sites in the promoter of the cognate structural genes (Pokorska et al., 2000; Nikolaev et al., 2003; Gómez et al., 2002). NirA is excluded from the nucleus in the absence of inducer (Berger et al., 2006; Bernreiter et al., 2007). UaY, on the other hand is, in our constructions, present in both the cytoplasm and the nucleus under non-induced conditions and excluded from the cytoplasm upon induction.

4. Conclusions

The purine utilization pathway is broadly conserved among the relatives of *A. nidulans*, and more widely in the Pezizomycotina, even if in this article we have limited ourselves to the analysis of the Eurotiales. Equally, the universal presence of a close orthologue of *uaY* among the Pezizomycotina argues for a strict conservation of the transcriptional regulation mechanism. Two facts emerge from the phylogenetic analysis. The first is the presence of para-

logues, probably with different specificity, of the specific fungal enzyme XanA (xanthine α-ketoglutarate dioxygenase) and AlX (allantoinase, (S)-allantoin amido hydrolase), arising most possibly from gene duplication of the ancestral purine utilizations genes. The second is the presence of genes, previously described in non-fungal species, arising from convergent evolution and able to catalyse the same steps as allantoinase and allantoicase (allantoate amidinohydroalase). In the case of allantoinase, the function of the strictly conserved homologue of the alternative allantoinase is obscure, as it occurs in organisms, which all comprise the classical allantoinase, which in *A. nidulans* is necessary and sufficient for the utilization of allantoin. For allantoicase, the situation is different and clearer, as the alternative enzyme occurs with very few exceptions in organisms where the classical allantoicase is absent. It is almost certain that the alternative fungal allantoicase originates from horizontal transmission from bacteria.

The intracellular distribution of the different enzymes was studied in *A. nidulans* and sequences in the data-bases suggest that is quite (but perhaps not completely) conserved in the Eurotiales. The production of uric acid is cytoplasmic, while the oxidation of uric acid to 2-oxo-4-hydroxy-4-carboxy-5-ureidoimidazonline occurs in the peroxisome. Surprisingly, the last step of the oxidation of urate to allantoin occurs in the cytoplasm. A cross-talk between cytoplasmic and peroxisomal enzyme activities is extant, because ureidoglycolate lyase is again a peroxisomal enzyme. We know little of the influx and efflux of metabolites from the peroxisome, their transport being compatible either with specific transporter proteins or with atypical permeability properties of the membrane and pore-forming complexes. The specificity of this mechanism(s) may be at the basis of this compartmentalization. However, mutations in the cognate genes have not been detected in genetic screens searching for mutants with dysfunctional peroxisomes, suggesting redundancy or essentiality of the cognate genes (Kunze and Hartig, 2013 and refs therein).

The pathway specific transcription factor UaY shows a hitherto undescribed pattern of nucleo-cytoplasmic shuffling: It is present in the nucleus and cytoplasm under non-inducing conditions, and is restricted to the nucleus under induced conditions. Even gross overproduction does not prevent complete, rapid, re-location to the nucleus, which implies the existence of a rather specific signaling mechanism at the root of this phenomenon.

Acknowledgments

We thank Prof. M. Hynes for providing us with the *pex* mutants, Prof. R. de Vries for providing *Aspergillus* strains from the JGI genome project, G. Langousis for initial efforts to construct strains relevant to this work and C. Gournas for fruitful discussions. K. Galanopoulou, M.E. Galinou, F. Borbolis and M. Karachaliou performed most of the experiments in this work as undergraduate students carrying their final year project in the laboratory of G. Diallinas. The work described was supported by the University of Athens. Work at Orsay was supported by the Université Paris-Sud, the CNRS and the Institut Universitaire de France.

Appendix A. Supplementary material

Supplementary data associated with this article can be found, in the online version, at http://dx.doi.org/10.1016/j.fgb.2014.06.005.

References

Allam, A.M., Elzainy, T.A., 1969. Degradation of xanthine by *Penicillium chrysogenum*. J. Gen. Microbiol. 56, 293–300.

Amrani, L., Primus, J., Glatigny, A., Arcangeli, L., Scazzocchio, C., Finnerty, V., 2000. Comparison of the sequences of the *Aspergillus nidulans* hxB and *Drosophila melanogaster* ma-l genes with nifS from *Azotobacter vinelandii* suggests a mechanism for the insertion of the terminal sulphur atom in the molybdopterin cofactor. Mol. Microbiol. 38, 114–125.

Apostolaki, A., Harispe, L., Calcagno-Pizarelli, A.M., Vangelatos, I., Sophianopoulou, V., Arst Jr., H.N., Peñalva, M.A., Amillis, S., Scazzocchio, C., 2012. *Aspergillus nidulans* CkiA is an essential casein kinase I required for delivery of amino acid transporters to the plasma membrane. Mol. Microbiol. 84, 530–549.

Berger, H., Pachlinger, R., Morozov, I., Goller, S., Narendja, F., Caddick, M., Strauss, J., 2006. The GATA factor AreA regulates localization and *in vivo* binding site occupancy of the nitrate activator NirA. Mol. Microbiol. 59, 433–446.

Bernreiter, A., Ramon, A., Fernández-Martínez, J., Berger, H., Araújo-Bazan, L., Espeso, E.A., Pachlinger, R., Gallmetzer, A., Anderl, I., Scazzocchio, C., Strauss, J., 2007. Nuclear export of the transcription factor NirA is a regulatory checkpoint for nitrate induction in *Aspergillus nidulans*. Mol. Cell. Biol. 27, 791–802.

Cecchetto, G., Richero, M., Oestreicher, N., Muro-Pastor, M.I., Pantano, S., Scazzocchio, C., 2012. Mutations in the basic loop of the Zn binuclear cluster of the UaY transcriptional activator suppress mutations in the dimerisation domain. Fungal Genet. Biol. 49, 731–743.

Cove, D.J., 1969. Evidence for a near limiting intracellular concentration of a regulator substance. Nature 224, 272–273.

Cultrone, A., Scazzocchio, C., Rochet, M., Montero-Morán, G., Drevet, C., Fernández-Martín, R., 2005. Convergent evolution of hydroxylation mechanisms in the fungal kingdom: molybdenum cofactor-independent hydroxylation of xanthine via alpha-ketoglutarate-dependent dioxygenases. Mol. Microbiol. 57, 276–290.

Cultrone, A., Domínguez, Y.R., Drevet, C., Scazzocchio, C., Fernández-Martín, R., 2007. The tightly regulated promoter of the xanA gene of *Aspergillus nidulans* is included in a helitron. Mol. Microbiol. 63, 1577–1587.

Darlington, A.J., Scazzocchio, C., 1968. Evidence for an alternative pathway of xanthine oxidation in *Aspergillus nidulans*. Biochim. Biophys. Acta 166, 569–571.

Darlington, A.J., Scazzocchio, C., Pateman, J.A., 1965. Biochemical and genetical studies of purine breakdown in Aspergillus. Nature 206, 599–600.

De la Riva, L., Badia, J., Aguilar, J., Bender, R.A., Baldoma, L., 2008. The hpx genetic system for hypoxanthine assimilation as a nitrogen source in *Klebsiella pneumoniae*: gene organization and transcriptional regulation. J. Bacteriol. 190, 7892–7903.

Diallinas, G., 2008. Aspergillus transporters. In: Osmani, A., Goldman, G.H. (Eds.), The Aspergilli. Genomics, Medical Applications, Biotechnology, and Research Methods. CRC Press, pp. 297–316.

Enroth, C., Eger, B.T., Okamoto, K., Nishino, T., Nishino, T., Pai, E.F., 2000. Crystal structures of bovine milk xanthine dehydrogenase and xanthine oxidase: structure-based mechanism of conversion. Proc. Natl. Acad. Sci. USA 97, 10723–10728.

Espeso, E.A., Cobeño, L., Arst Jr., H.N., 2005. Discrepancies between recombination frequencies and physical distances in *Aspergillus nidulans*: implications for gene identification. Genetics 171, 835–838.

Etxebeste, O., Markina-Iñarrairaegui, A., Grazia, A., Herrero-García, E., Ugalde, U., Espeso, E.A., 2009. Kap1, a non-essential member of the Pse1p/Imp5 karyopherin family, controls colonial and asexual development in *Aspergillus nidulans*. Microbiology 155, 3934–3945.

Gill, G., Ptashne, M., 1988. Negative effect of the transcriptional activator GAL4. Nature 334, 721–724.

Glatigny, A., Scazzocchio, C., 1995. Cloning and molecular characterization of hxA, the gene coding for the xanthine dehydrogenase (purine hydroxylase I) of *Aspergillus nidulans*. J. Biol. Chem. 270, 3534–3550.

Gómez, D., Cubero, B., Cecchetto, G., Scazzocchio, C., 2002. PrnA, a Zn2Cys6 activator with a unique DNA recognition mode, requires inducer for in vivo binding. Mol. Microbiol. 44, 585–597.

Gómez, D., García, I., Scazzocchio, C., Cubero, B., 2003. Multiple GATA sites: protein binding and physiological relevance for the regulation of the proline transporter gene of *Aspergillus nidulans*. Mol. Microbiol. 50, 277–289.

Gournas, C., Amillis, S., Vlanti, A., Diallinas, G., 2010. Transport-dependent endocytosis and turnover of a uric acid-xanthine permease. Mol. Microbiol. 75, 246–260.

Gournas, C., Oestreicher, N., Amillis, S., Diallinas, G., Scazzocchio, C., 2011. Completing the purine utilisation pathway of *Aspergillus nidulans*. Fungal Genet. Biol. 48, 840–848.

Gründlinger, M., Yasmin, S., Lechner, B.E., Geley, S., Schrettl, M., Hynes, M., Haas, H., 2013. Fungal siderophore biosynthesis is partially localized in peroxisomes. Mol. Microbiol. 88, 862–875.

Hamari, Z., Amillis, S., Drevet, C., Apostolaki, A., Vágvölgyi, C., Diallinas, G., Scazzocchio, C., 2009. Convergent evolution and orphan genes in the Fur4p-like family and characterization of a general nucleoside transporter in *Aspergillus nidulans*. Mol. Microbiol. 73, 43–57.

Hayashi, S., Fujiwara, S., Noguchi, T., 2000. Evolution of urate-degrading enzymes in animal peroxisomes. Cell Biochem. Biophys. 32, 123–129.

Hilliker, A.J., Duyf, B., Evans, D., Phillips, J.P., 1992. Urate-null rosy mutants of *Drosophila melanogaster* are hypersensitive to oxygen stress. Proc. Natl. Acad. Sci. USA 89, 4343–4347.

Hynes, M.J., Murray, S.L., Khew, G.S., Davis, M.A., 2008. Genetic analysis of the role of peroxisomes in the utilization of acetate and fatty acids in *Aspergillus nidulans*. Genetics 178, 1355–1369.

Ito, M., Nakamura, M., Kato, S., Ogawa, H., Takagi, Y., 1991. Structural analysis of the rat uricase gene and evidence that lysine 164 is involved in the substrate-binding site of the enzyme. Adv. Exp. Med. Biol. 309, 377–381.

Karachaliou, M., Amillis, S., Evangelinos, M., Kokotos, A.C., Yalelis, V., Diallinas, G., 2013. The arrestin-like protein ArtA is essential for ubiquitination and

endocytosis of the UapA transporter in response to both broad-range and specific signals. Mol. Microbiol. 88, 301–317.
Kim, K., Kim, M.I., Chung, J., Ahn, J.H., Rhee, S., 2009. Crystal structure of metal-dependent allantoinase from *Escherichia coli*. J. Mol. Biol. 387, 1067–1074.
Koukaki, M., Giannoutsou, E., Karagouni, A., Diallinas, G., 2003. A novel improved method for *Aspergillus nidulans* transformation. J. Microbiol. Methods 55, 687–695.
Kunze, M., Hartig, A., 2013. Permeability of the peroxisomal membrane: lessons from the glyoxylate cycle. Front. Physiol. 4, 204.
Lehninger, A.L., 1981. Biochemistry, second ed. Worth, New York, pp. 729–747.
Lewis, N.J., Scazzocchio, C., 1977. The genetic control of molybdoflavoproteins in *Aspergillus nidulans*. A xanthine dehydrogenase I half-molecule in cnx-mutant strains of *Aspergillus nidulans*. Eur. J. Biochem. 76, 441–446.
Lewis, N.J., Hurt, P., Sealy-Lewis, H.M., Scazzocchio, C., 1978. The genetic control of the molybdoflavoproteins in *Aspergillus nidulans*. IV. A comparison between purine hydroxylase I and II. Eur. J. Biochem. 91, 311–316.
Li, L., Hu, X., Xia, Y., Xiao, G., Zheng, P., Wang, C., 2014. Linkage of oxidative stress and mitochondrial dysfunctions to spontaneous culture degeneration in *Aspergillus nidulans*. Mol. Cell. Proteomics 13, 449–461.
Liu, T.D., Marzluf, G.A., 2004. Characterization of pco-1, a newly identified gene which regulates purine catabolism in Neurospora. Curr. Genet. 46, 213–227.
Liu, W., Mellado, L., Espeso, E.A., Heather, M., Sealy-Lewis, H.M., 2014. In *Aspergillus nidulans* the suppressors suaA and suaC code for release factors eRF1 and eRF3 and suaD codes for a glutamine tRNA. G3 (Bethesda) 4, 1047–1057.
Mei, D.A., Gross, G.J., Nithipatikom, K., 1996. Simultaneous determination of adenosine, inosine, hypoxanthine, xanthine, and uric acid in microdialysis samples using microbore column high-performance liquid chromatography with a diode array detector. Anal. Biochem. 238, 34–39.
Montero-Morán, G.M., Li, M., Rendòn-Huerta, E., Jourdan, F., Lowe, D.J., Stumpff-Kane, A.W., Feig, M., Scazzocchio, C., Hausinger, R.P., 2007. Purification and characterization of the FeII- and alpha-ketoglutarate-dependent xanthine hydroxylase from *Aspergillus nidulans*. Biochemistry 46, 5293–5304.
Moriwaki, Y., Yamamoto, T., Higashino, K., 1999. Enzymes involved in purine metabolism – a review of histochemical localization and functional implications. Histol. Histopathol. 14, 1321–1340.
Müller, M., Moller, K.M., 1969. Urate oxidase and its association with peroxisomes in Acanthamoeba sp. Eur. J. Biochem. 9, 424–430.
Nayak, T., Szewczyk, E., Oakley, C.E., Osmani, A., Ukil, L., Murray, S.L., Hynes, M.J., Osmani, S.A., Oakley, B.R., 2006. A versatile and efficient gene-targeting system for *Aspergillus nidulans*. Genetics 172, 1557–1566.
Nikolaev, I., Cochet, M.F., Felenbok, B., 2003. Nuclear import of zinc binuclear cluster proteins proceeds through multiple, overlapping transport pathways. Eukaryot. Cell 2, 209–221.
Oestreicher, N., Scazzocchio, C., 1993. Sequence, regulation, and mutational analysis of the gene encoding urate oxidase in *Aspergillus nidulans*. J. Biol. Chem. 268, 23382–23389.
Oestreicher, N., Scazzocchio, C., 1995. A single amino acid change in a pathway-specific transcription factor results in differing degrees of constitutivity, hyperinducibility and derepression of several structural genes. J. Mol. Biol. 249, 693–699.
Oestreicher, N., Scazzocchio, C., 2009. Phenotypes of mutations in the 5′-UTR of a limiting transcription factor in *Aspergillus nidulans* can be accounted for by translational inhibition and leaky scanning. Genetics 181, 1261–1272.
Oestreicher, N., Sealy-Lewis, H.M., Scazzocchio, C., 1993. Characterisation, cloning and integrative properties of the gene encoding urate oxidase in *Aspergillus nidulans*. Gene 132, 185–192.
Oestreicher, N., Scazzocchio, C., Suárez, T., 1997. Mutations in a dispensable region of the UaY transcription factor of *Aspergillus nidulans* differentially affect the expression of structural genes. Mol. Microbiol. 24, 1189–1199.
Pantazopoulou, A., Lemuh, N.D., Hatzinikolaou, D.G., Drevet, C., Cecchetto, G., Scazzocchio, C., Diallinas, G., 2007. Differential physiological and developmental expression of the UapA and AzgA purine transporters in *Aspergillus nidulans*. Fungal Genet. Biol. 44, 627–640.
Peñalva, M.A., 2005. Tracing the endocytic pathway of *Aspergillus nidulans* with FM4-64. Fungal Genet. Biol. 42, 963–975.
Percudani, R., Carnevali, D., Puggioni, V., 2013. Ureidoglycolate hydrolase, amidohydrolase, lyase: how errors in biological databases are incorporated in scientific papers and vice versa. Database (Oxford), 2013:bat071.
Petriv, O.I., Tang, L., Titorenko, V.I., Rachubinski, R.A., 2004. A new definition for the consensus sequence of the peroxisome targeting signal type 2. J. Mol. Biol. 341, 119–134.
Pokorska, A., Drevet, C., Scazzocchio, C., 2000. The analysis of the transcriptional activator PrnA reveals a tripartite nuclear localisation sequence. J. Mol. Biol. 298, 585–596.
Pope, S.D., Chen, L.L., Stewart, V., 2009. Purine utilization by *Klebsiella oxytoca* M5al: genes for ring-oxidizing and -opening enzymes. J. Bacteriol. 191, 1006–1017.
Puggioni, V., Dondi, A., Folli, C., Shin, I., Rhee, S., Percudani, R., 2014. Gene context analysis reveals functional divergence between hypothetically equivalent enzymes of the purine–ureide pathway. Biochemistry 53, 735–745.
Ramazzina, I., Folli, C., Secchi, A., Berni, R., Percudani, R., 2006. Completing the uric acid degradation pathway through phylogenetic comparison of whole genomes. Nat. Chem. Biol. 2, 144–148.
Ramazzina, I., Cendron, L., Folli, C., Berni, R., Monteverdi, D., Zanotti, G., Percudani, R., 2008. Logical identification of an allantoinase analog (puuE) recruited from polysaccharide deacetylases. J. Biol. Chem. 283, 23295–23304.
Raymond, S., Tocilj, A., Ajamian, E., Li, Y., Hung, M.N., Matte, A., Cygler, M., 2005. Crystal structure of ureidoglycolate hydrolase (AllA) from *Escherichia coli* O157:H7. Proteins 61, 454–459.
Roberts, T., Martinelli, S., Scazzocchio, C., 1979. Allele specific, gene unspecific suppressors in *Aspergillus nidulans*. Mol. Gen. Genet. 177, 57–64.
Scazzocchio, C., 1980. The genetics of the molybdenum-containing enzymes. In: Coughlan, M. (Ed.), Molybdenum and Molybdenum-containing Enzymes. Pergamon Press, Oxford, New York, Toronto, Sydney, Paris, Frankfurt, pp. 487–515.
Scazzocchio, C., 1994. The purine degradation pathway, genetics, biochemistry and regulation. Prog. Ind. Microbiol. 29, 221–257.
Scazzocchio, C., Darlington, A.J., 1968. The induction and repression of the enzymes of purine breakdown in *Aspergillus nidulans*. Biochim. Biophys. Acta 166, 557–568.
Scazzocchio, C., Holl, F.B., Foguelman, A.I., 1973. The genetic control of molybdoflavoproteins in *Aspergillus nidulans*. Allopurinol-resistant mutants constitutive for xanthine-dehydrogenase. Eur. J. Biochem. 36, 428–445.
Scazzocchio, C., Sdrin, N., Ong, G., 1982. Positive regulation in a eukaryote, a study of the uaY gene of *Aspergillus nidulans*: I. Characterization of alleles, dominance and complementation studies, and a fine structure map of the uaY–oxpA cluster. Genetics 100, 185–208.
Sealy-Lewis, H.M., Scazzocchio, C., Lee, S., 1978. A mutation defective in the xanthine alternative pathway of *Aspergillus nidulans*: its use to investigate the specificity of *uaY* mediated induction. Mol. Gen. Genet. 164, 303–308.
Suárez, T., Oestreicher, N., Peñalva, M.A., Scazzocchio, C., 1991. Molecular cloning of the *uaY* regulatory gene of *Aspergillus nidulans* reveals a favoured region for DNA insertions. Mol. Gen. Genet. 230, 369–375.
Suárez, T., de Queiroz, M.V., Oestreicher, N., Scazzocchio, C., 1995. The sequence and binding specificity of UaY, the specific regulator of the purine utilization pathway in *Aspergillus nidulans*, suggest an evolutionary relationship with the PPR1 protein of *Saccharomyces cerevisiae*. EMBO J. 14, 1453–1467.
Takada, Y., Tsukiji, N., 1987. Peroxisomal localization and activation by bivalent metal ions of ureidoglycolate lyase, the enzyme involved in urate degradation in *Candida tropicalis*. J. Bacteriol. 169, 2284–2286.
Tavernarakis, N., Thireos, G., 1995. Transcriptional interference caused by GCN4 overexpression reveals multiple interactions mediating transcriptional activation. Mol. Gen. Genet. 247, 571–578.
Tilburn, J., Scazzocchio, C., Taylor, G.G., Zabicky-Zissman, J.H., Lockington, R.A., Davies, R.W., 1983. Transformation by integration in *Aspergillus nidulans*. Gene 26, 205–221.
Valdez-Taubas, J., Harispe, L., Scazzocchio, C., Gorfinkiel, L., Rosa, A.L., 2004. Ammonium-induced internalisation of UapC, the general purine permease from *Aspergillus nidulans*. Fungal Genet. Biol. 41, 42–51.
Vogels, G.D., Van der Drift, C., 1976. Degradation of purines and pyrimidines by microorganisms. Bacteriol. Rev. 40, 403–468.
Yu, R., Schellhorn, H.E., 2013. Recent applications of engineered animal antioxidant deficiency models in human nutrition and chronic disease. J. Nutr. 143, 1–11.
Zanotti, G., Cendron, L., Ramazzina, I., Folli, C., Percudani, R., Berni, R., 2006. Structure of zebra fish HIUase: insights into evolution of an enzyme to a hormone transporter. J. Mol. Biol. 363, 1–9.